Stochastic-trajectories and nonPoisson kinetics in single-molecule spectroscopy

Vladimir Chernyak, Michael Schulz, and Shaul Mukamel
Department of Chemistry and Rochester Theory Center for Optical Science and Engineering, University of Rochester, Rochester, New York 14627

(Received 1 June 1999; accepted 29 July 1999)

Microscopic correlation-function expressions for the stochastic evolution observed in single molecule spectroscopy are derived using Liouville-space projection operators. The kinetics of a multilevel quantum system coupled to a single collective overdamped Brownian-oscillator coordinate is exactly mapped onto a continuous-time-random-walk (CTRW) involving the transition states(curve-crossing points). Closed expressions are derived for the stochastic trajectories and the nonPoissonian distribution of number of flips. When the oscillator relaxation is fast compared with the reaction rates, the waiting time distribution becomes exponential and the standard Poisson kinetics is recovered. © *1999 American Institute of Physics.* [S0021-9606(99)01340-9]

I. INTRODUCTION

Recent advances in fluorescence detection and microscopy allow the studies of single molecules in complex condensed phase environments at cryogenic as well as room temperatures.[1–7] Single-molecule spectroscopy (SMS) provides much more detailed microscopic information on the molecule under study and its coupling to the environment, than standard bulk measurements. The technique eliminates ensemble averaging and disorder effects from the outset, without involving spectroscopically-selective methods such as photon echo[8] or hole burning.[9] SMS allows to probe motions which are slow compared to the fluorescence decay time, which is not possible using conventional bulk spectroscopy.

SMS signals show stochastic behavior which originates from translational[10–12] and rotational[13] diffusion, spectral fluctuations,[14] conformational motions,[15] and chemical-changes-induced fluorescence blinking.[16,17] Detailed information on these motions can be obtained through a statistical analysis of the stochastic trajectories. Stochastic models of various kinds[18–20] including random jump models[21] as well as continuous-time random walks[22] have been used for the interpretation of SMS experiments.

In this article we compute the stochastic SMS trajectories for chemical reactions coupled to a slow solvation coordinate. Apart from providing detailed information on molecular dynamics, SMS also has the capacity to clarify some fundamental questions regarding the microscopic quantum description of single objects.[23–28] The following issues will be addressed as well: what is the relation between the microscopic models which describe the dynamics of a system in terms of Liouville space evolution of the density matrix? Does the density matrix merely represent ensemble averages or does it also provide a powerful and useful tool for understanding the dynamics of single objects?

Kinetic (rate) equations provide a simple framework for the interpretation of chemical dynamics. When this level of theoretical description applies, the statistics of stochastic trajectories is strictly Poissonian and carries no additional information beyond the macroscopic rate constants.[16,17] Microscopically, rate equations hold when all other degrees of freedom are fast compared with the observed kinetic time scales. Once the kinetic variables are coupled to some slow degrees of freedom, the theoretical description must include them explicitly, and the simple kinetic equations no longer hold. Under these circumstances the stochastic trajectories observed in SMS provide an important source of additional microscopic information about the system. A common model is to couple a multilevel system to an overdamped macroscopic slow coordinate described by the Smoluchowski equation.[29–31] In general, solving these equations requires computing the evolution of coupled nuclear wavepackets.[32] One of the interesting results of this article is that when the reactions occur at well localized nuclear configurations, the stochastic evolution can be rigorously mapped onto the continuous time random walk (CTRW) model.[33,34] In ordinary random walks, the walker jumps between different sites at fixed regular time intervals. Instead, the CTRW adds a distribution of waiting times between successive jumps. The model was first proposed by Montroll and Weiss.[33] Extensions and further developments were made by Klafter, Zumofen, and Shlesinger.[22,34] Hopping among the curve-crossing points associated with each pair of states results in the discrete CTRW. The distribution of waiting times originates from the evolution of the slow coordinate once it is eliminated from the description. Rather than solving a set of coupled partial differential equations for nuclear wavepackets, we obtain a random walk where the slow dynamics is rigorously incorporated into the waiting time distribution. One technical difference from the standard CTRW is that we need several waiting time distributions, not just one. When the nuclear coordinate becomes fast, we recover the simple kinetic equations with Poisson statistics.

In Sec. II we start with one of the basic postulates of quantum mechanics due to von Neumann to derive general expressions for the probability to obtain a certain result in a

sequence of measurements in terms of a Liouville space multitime correlation function. It is important to note that the stochastic model describes the probability of getting a certain result in a sequence of measurements, rather than the free dynamics of the unperturbed system.[28] The result of a sequence of measurements will hereafter be referred to as a stochastic trajectory. The probability of a given trajectory is expressed in terms of a multitime Liouville-space correlation function of the unperturbed system. This establishes a firm connection between the microscopic and stochastic descriptions of SMS, and provides a prescription for computing the stochastic trajectories and their statistical properties. In Sec. III we apply this approach to a kinetic model of L levels coupled to a single overdamped Brownian mode. We derive the stochastic model corresponding to this microscopic model, and show that it corresponds to a continuous-time-random-walk. Expressions for the distribution of the number of flips are derived in Appendix A. In Sec. IV we consider the simplest case of two level kinetics. Numerical calculations which illustrate the nonPoisson nature of the stochastic trajectories, and a brief summary are given in Sec. V.

II. CORRELATION-FUNCTION EXPRESSIONS FOR THE EFFECTIVE STOCHASTIC MODELS

In this section we derive correlation-function expressions which make it possible to interpret SMS signals starting with a fully microscopic description of the system. Because of the quantum nature of microscopic objects, one can only predict the probability of a certain outcome in a set of measurements rather than the actual result.[35] This probability can be expressed in terms of Liouville-space correlation functions using the following postulate due to von Neumann, which reflects the Copenhagen interpretation of quantum mechanics.[36] A measurement with L possible outcomes can be described by decomposing the Hilbert space of states V of a quantum system into a direct sum $V=V_1\oplus V_2\oplus\cdots\oplus V_L$ where the space V_j $(j=1,2,\ldots,L)$ corresponds to the jth outcome of a measurement. Let P_j be the projection operator associated with V_j. According to von Neumann, for a system whose state is described by a wavefunction ψ, the probability to get the result j in a measurement is given by $|\langle\psi|\hat{P}_j|\psi\rangle|^2$ and after the measurement the system has the wavefunction $\hat{P}_j|\psi\rangle|\langle\psi|\hat{P}_j|\psi\rangle|^{-1}$. If we repeat the same measurement at times $\tau_1,\tau_2\ldots\tau_N$, apply von Neumann's principle N times, and combine it with the time-dependent Schrodinger equation, we get for the probability $P(j_N,\ldots,j_1;\tau_N,\ldots,\tau_1)$ to obtain the results $j_1,\ldots,j_N$ in these measurements:

$$P(j_N,\ldots,j_1;\tau_N,\ldots,\tau_1)=\langle\psi|\hat{P}_{j_1}e^{iHt_1}\ldots e^{iHt_{N-1}}\hat{P}_{j_N}e^{-iHt_{N-1}}\ldots e^{-iHt_1}\hat{P}_{j_1}|\psi\rangle, \tag{2.1}$$

where $|\psi\rangle$ is the initial wavefunction and $t_m\equiv\tau_{m+1}-\tau_m$ is the nth time interval between successive measurements. This distribution, normalized as $\Sigma_{j_1,\ldots,j_N}P(j_N,\ldots,j_1;\tau_N,\ldots,\tau_1)=1$, can be recast in Liouville-space form

$$\begin{aligned}P(j_N,\ldots,j_1;\tau_N,\ldots,\tau_1)&=\langle\mathcal{P}_{j_N}(\tau_n)\ldots\mathcal{P}_{j_1}(\tau_1)\rangle\\&\equiv\mathrm{Tr}[\mathcal{P}_{j_N}e^{-i\tilde{L}t_{N-1}}\mathcal{P}_{j_{N-1}}\ldots e^{-i\tilde{L}t_1}\mathcal{P}_{j_1}\tilde{\rho}],\end{aligned} \tag{2.2}$$

where $\tilde{\rho}=|\psi\rangle\langle\psi|$ is the equilibrium density matrix, $\tilde{L}=[H,]$ is the Liouville operator, and $\mathcal{P}_j(\rho)\equiv\hat{P}_j\rho\hat{P}_j$ are projection superoperators. Equation (2.2) expresses the probability $P(j_N,\ldots,j_1;\tau_N,\ldots,\tau_1)$ as a Liouville-space correlation function of the projection superoperators $\mathcal{P}_j$ and allows to interpret the SMS signals in terms of Liouville-space dynamics. Even though we have derived Eq. (2.2) for a density matrix $\tilde{\rho}$ that corresponds to a pure state $|\psi\rangle$, it also holds in the more general case of a mixed state. This can be obtained by starting in a pure state in an extended (system and bath) space. By then integrating out the bath coordinates assuming that the projection operators $\hat{P}_j$ do not depend on the bath, we recover Eq. (2.2), where $\tilde{\rho}$ now represents the reduced system density matrix.

Consider an experiment involving repeated measurements separated by a fixed time interval $t_j\equiv\tau_{j+1}-\tau_j=\Delta\tau$. Introducing the operators $\mathcal{U}_{ij}\equiv\mathcal{P}_i\exp(-i\tilde{L}\Delta\tau)\mathcal{P}_j$ we can recast Eq. (2.2) in the form:

$$P(j_N,\ldots,j_1)=\mathrm{Tr}\{\mathcal{U}_{j_Nj_{N-1}}\ldots\mathcal{U}_{j_2j_1}\tilde{\rho}\}. \tag{2.3}$$

Equation (2.3) can be viewed as the probability of a trajectory determined by a sequence $j_N,\ldots,j_1$ for a stochastic model defined on a lattice. The stochastic model described by Eq. (2.3) and formed by the possible outcomes j_k provides a continuous limit representation as long as the time interval $\Delta\tau$ is kept short compared with the Liouville-space dynamics time scale. This implies that the flips are rare and the description of the stochastic dynamics is given by the probability $P_f(j_N,\ldots,j_0;\tau_N,\ldots,\tau_1)$ that the flips occur at times $\tau_1,\ldots,\tau_N$ while at time τ_k the system flips from j_{k-1} to j_k. Typically $n\ll N$ where n is the number of flips. Expanding $\mathcal{U}_{jj}\approx I+(\Delta\tau)\mathcal{L}_j$, $\mathcal{U}_{ij}\approx(\Delta\tau)v_{ij}$ for $i\neq j$ the probability P_f finally assumes the form:

$$P_f(j_n,\ldots,j_0;\tau_n',\ldots,\tau_1')=\int_{\tau_1-\Delta\tau}^{\tau_1}d\tau_1'\ldots\int_{\tau_n-\Delta\tau}^{\tau_n}d\tau_n'P_s(j_n,\ldots,j_0;\tau_n',\ldots,\tau_1'), \tag{2.4}$$

with the probability density

$$P_s(j_n,\ldots,j_0;\tau_n,\ldots,\tau_1)=\mathrm{Tr}\{e^{-i\mathcal{L}_{j_n}(\tau-\tau_n)}v_{j_nj_{nN-1}}\ldots e^{-i\mathcal{L}_{j_1}(\tau_2-\tau_1)}v_{j_1j_0}e^{-i\mathcal{L}_{j_0}\tau_1}\tilde{\rho}\}. \tag{2.5}$$

Equation (2.5) relates the stochastic model of SMS signals to microscopic quantities. P_s can be interpreted as the probability of a continuous stochastic trajectory whereas P_f is its regularized form.

III. CONTINUOUS-TIME-RANDOM-WALKS FOR MULTISTATE KINETICS

In this section we apply Eq. (2.5) to derive a stochastic model for SMS starting with a microscopic model of an L-level quantum system coupled linearly to an overdamped Browninan oscillator with an arbitrary relaxation time scale. We assume that a measurement determines that the system occupies one of the L levels $|n\rangle$, which are not eigenstates of the system Hamiltonian H_s:

$$H_s=\sum_n E_n|n\rangle\langle n|+\sum_{nm}^{n\neq m} J_{nm}|n\rangle\langle m|. \tag{3.1}$$

We further assume a diagonal coupling to a harmonic bath described by the Hamiltonian:

$$H_{\rm int}=-\sum_n q^{(n)}|n\rangle\langle n|, \tag{3.2}$$

where $q^{(n)}$ denote the set of collective bath coordinates. All relevant information about the bath is contained in the matrix of spectral densities[37,32,38]

$$C_{ij}(\omega)=\frac{i}{2}\int_{-\infty}^{\infty}d\tau\exp(i\omega\tau)\langle[q^{(i)}(\tau),q^{(j)}(0)]\rangle. \tag{3.3}$$

The Liouville-space dynamics is described by the evolution of the wavepackets $\rho_{ij}(q)$ where q represent the complete set of bath variables. q can be viewed as a set of collective relevant bath variables and the coordinates $q^{(n)}$ in Eq. (3.2) are linear combinations of the components of q. The number of collective coordinates (i.e., the number of components of q) needed for a reasonable reduced description is uniquely determined by the matrix of spectral densities $C_{ij}(\omega)$ as well as the temperature.[32]

Below we consider a model which includes a single overdamped Brownian oscillator mode, where the collective coordinates $q^{(n)}$ responsible for the coupling are given by $q^{(n)}=2\eta d_n q$ and the spectral density is:

$$C_{ij}(\omega)=d_i d_j\frac{2\eta\Lambda}{\omega^2+\Lambda^2}. \tag{3.4}$$

Here Λ is the relaxation rate of q whereas η denotes its coupling strength with the multilevel system. In the high-temperature ($\Lambda\ll k_BT$) limit, the dynamics can be described by the evolution of wavepackets $\rho_{ij}(q)$ which only depend on a single collective coordinate q.

The effective Liouville operator which describes the propagation of the wavepackets in the absence of system-bath coupling is represented by the Smoluchowski operator [Eq. (3.8)]. In the spectral-diffusion ($\Lambda\ll\sqrt{2\eta k_BT}$) limit, the off-diagonal (coherence) wavepackets [i.e., $\rho_{ij}(q)$ for $i\neq j$] can be eliminated from the equations of motion, resulting in a closed system of equations for the diagonal (population) wavepackets:[29]

$$\frac{d\rho_{mm}(q,\tau)}{d\tau}=\mathcal{L}_m^{(0)}\rho_{mm}(q,\tau)+\sum_n \kappa_{mn}\overline{\rho}(q-q_{mn})\times[\rho_{nn}(q,\tau)-\rho_{mm}(q,\tau)], \tag{3.5}$$

where $\overline{\rho}=\delta(q)$, q_{mn} are the crossing points of the potential surfaces of states $|n\rangle$ and $|m\rangle$

$$q_{mn}=q_{nm}=\frac{E_m-E_n}{2\eta(d_m-d_n)}, \tag{3.6}$$

κ_{mn} are the transition rates at the crossing points:

$$\kappa_{mn}=\kappa_{nm}=\frac{2\pi|J_{mn}|^2}{2\eta|d_m-d_n|}, \tag{3.7}$$

and $\mathcal{L}_m^{(0)}$ is the Smoluchowski operator for the population wavepacket ρ_{mm}:

$$\mathcal{L}_m^{(0)}=\Lambda\frac{\partial}{\partial q}\left[(q-d_m)+\left(\frac{k_BT}{2\eta}\right)\frac{\partial}{\partial q}\right]. \tag{3.8}$$

To identify the operators $\mathcal{L}_j$ and v_{ij} required for the evaluation of Eq. (2.5) we need to start with a wavepacket $\rho_{jj}(q)$, propagate it for a short time interval $\Delta\tau$, and find these operators from the conditions

$$\begin{aligned}&\rho_{jj}(q,\tau+\Delta\tau)-\rho_{jj}(q,\tau)=(\Delta\tau)\mathcal{L}_j\rho_{jj}(q,\tau),\\&\rho_{ii}(q,\tau+\Delta\tau)=(\Delta\tau)v_{ij}\rho_{jj}(q,\tau).\end{aligned} \tag{3.9}$$

$\Delta\tau$ is taken to be short compared to the time scale of the evolution of the population wavepackets, and only terms linear in $\Delta\tau$ should be retained in the l.h.s.

Combining Eq. (3.9) with Eq. (3.5) immediately yields

$$\begin{aligned}&\mathcal{L}_j=\mathcal{L}_j^{(0)}-\sum_n^{n\neq j}\kappa_{jn}\overline{\rho}(q-q_{jn}),\\&v_{ij}=\kappa_{ij}\overline{\rho}(q-q_{ij}).\end{aligned} \tag{3.10}$$

Equation (3.10) together with Eq. (2.5) determine the stochastic model for SMS corresponding to the microscopic model defined by Eqs. (3.1)–(3.4). For practical applications we can describe the wavepackets $\overline{\rho}(q)$ in Eq. (3.10) as narrow-Gaussians rather than δ-functions. The finite width of $\overline{\rho}(q)$ which may result from eliminating fast bath degrees of freedom weakly coupled to the system frees the theory from any divergences.

The solution of Eq. (3.5) is carried out in three steps. First, nonadiabatic transitions are neglected. The Smoluchowski equation with $\mathcal{L}_m^{(0)}$ is solved analytically in each state, resulting in N Gaussian Green functions G. In the second step we add the term representing the leaking out from each state (but still neglect the return). This results in $\mathcal{L}_j$ [Eq. (3.10)]. This gives in an $(L-1)\times(L-1)$ matrix $W^{(j)}$ for each state, representing the waiting time distribution between each pair of crossing points involving that state. $W^{(j)}$ for each state of j is expressed in a closed form using G. Finally we consider the full Smoluchowski equations, express the resulting stochastic trajectories using $W^{(j)}$, and show that they represent a continuous-time-random-walk.

We start with the first step. According to Eq. (2.5), the evolution of the system between flips in state $|j\rangle$ is determined by the effective Liouville operator $\mathcal{L}_j$ [Eq. (3.10)], which consists of two terms. The first term $\mathcal{L}_j^{(0)}$ constitutes the Smoluchowski operator which describes the diffusion of the oscillator coordinate whereas the second term is related

to the loss of the population at state $|j\rangle$ which occurs at the crossing points q_{jn}. The evolution with the operators $\mathcal{L}_j^{(0)}$ is described by the Green functions $G^{(j)}(q,q';\tau)$ of the Smoluchowski equations, defined as the solutions of

$$\frac{dG^{(j)}(q,q';\tau)}{d\tau}-\mathcal{L}_0^{(j)}G^{(j)}(q,q';\tau)=0, \tag{3.11}$$

with the initial conditions

$$G^{(j)}(q,q';,0)=\overline{\rho}(q-q'). \tag{3.12}$$

In our model the kinetics is fully determined by the values of the Green functions $G^{(j)}(q,q';\tau)$ at the crossing points where the populations can change. This yields a set of $(L-1)\times(L-1)$ matrices $G_{mn}^{(j)}(\tau)$ with $m,n=1,2\ldots,j-1,j+1,\ldots L$:

$$G_{mn}^{(j)}(\tau)\equiv G^{(j)}(q_{mj},q_{nj};\tau), \tag{3.13}$$

which have the form

$$G_{mn}^{(j)}(\tau)=\frac{1}{\sqrt{2\pi}\sigma(\tau)}\exp\left\{-\frac{[q_{mj}-x_{nj}(\tau)]^2}{2\sigma^2(\tau)}\right\}, \tag{3.14}$$

with

$$\sigma^2(\tau)\equiv\left(\frac{k_BT}{2\eta}\right)-\left[\left(\frac{k_BT}{2\eta}\right)-\sigma_0^2\right]e^{-2\Lambda\tau}, \tag{3.15}$$

$$x_{nj}(\tau)\equiv d_j-(d_j-q_{nj})e^{-\Lambda\tau}. \tag{3.16}$$

In Eq. (3.15) σ_0 is a regularization parameter, representing a finite width at $\tau=0$, and the wavepacket $\overline{\rho}$ in Eq. (2.5) has the form

$$\overline{\rho}(q)=\frac{1}{\sqrt{2\pi}\sigma_0}\exp\left(-\frac{q^2}{2\sigma_0^2}\right), \tag{3.17}$$

which becomes a δ-function in the limit $\sigma_0=0$.

Turning to the second step, we consider the following sequence of events (history): the system jumps from $|j_{k-2}\rangle$ to state $|j_{k-1}\rangle$, remains in that state for the time interval τ, and finally jumps to state $|j_k\rangle$. It follows from Eq. (2.5) that the probability for this sequence is

$$\hat{W}_{j_kj_{k-2}}^{(j_{k-1})}(\tau)\equiv\mathrm{Tr}[v_{j_kj_{k-1}}\exp(-i\mathcal{L}_{j_{k-1}}\tau)\overline{\rho}_{j_{k-1}j_{k-2}}], \tag{3.18}$$

where $\overline{\rho}_{j_{k-1}j_{k-2}}(q)=\overline{\rho}(q-q_{j_{k-1}j_{k-2}})$. The operator in the r.h.s. of Eq. (3.18) can be expressed in terms of the Green function of the Smoluchowski equation [Eq. (3.14)] by switching to the frequency representation, which yields:

$$\hat{W}^{(j)}(\omega)\equiv\hat{\kappa}^{(j)}\hat{G}^{(j)}(\omega)[I+\hat{\kappa}^{(j)}\hat{G}^{(j)}(\omega)]^{-1}, \tag{3.19}$$

where $\hat{\kappa}_{mn}^{(j)}\equiv\delta_{mn}\kappa_{mj}$ and we adopt the following convention for the Fourier transform:

$$W^{(j)}(\tau)=\int_{-\infty}^{\infty}\frac{d\omega}{2\pi}\hat{W}^{(j)}(\omega)\exp(-i\omega\tau). \tag{3.20}$$

Using Eq. (3.10), the probability for a stochastic trajectory [Eq. (2.5)] becomes:

$$\begin{aligned}P_s(j_n,\ldots,j_0;\tau_n,\ldots,\tau_1)&=\hat{W}_{j_nj_{n-1}}^{(0)}(\tau-\tau_n)\hat{W}_{j_nj_{n-2}}^{(j_{n-1})}(\tau_n-\tau_{n-1})\ldots\\&\times W_{j_2j_0}^{(j_1)}(\tau_2-\tau_1)\mathcal{D}_{j_1j_0}^{(0)}(\tau_1).\end{aligned} \tag{3.21}$$

The first factor from the right $\mathcal{D}_{j_1j_2}^{(0)}(\tau)$ is the probability to stay in state $|j_0\rangle$ for time τ and jump to state $|j_1\rangle$. We denote it the doorway function

$$\mathcal{D}_{j_1j_0}^{(0)}(\tau)\equiv\mathrm{Tr}[v_{j_1j_0}\exp(-i\mathcal{L}_{j_0}\tau)\tilde{\rho}^{(j_0)}], \tag{3.22}$$

and $\tilde{\rho}^{(j_0)}$ is the $\rho_{j_0j_0}(q)$ component of the stationary solution of Eq. (3.5). Following that, Eq. (3.21) contains a series of $n-1$ evolution periods related to the waiting time distributions [Eq.(3.18)]. Finally the last period is represented by the window function $W_{j_nj_{n-1}}^{(0)}(\tau)$ which gives the probability of state $|j_n\rangle$ to survive during the time τ, provided it was created by a flip from state $|j_{n-1}\rangle$,

$$W_{j_nj_{n-1}}^{(0)}(\tau)\equiv\mathrm{Tr}[\exp(-i\mathcal{L}_{j_n}\tau)\overline{\rho}_{j_nj_{n-1}}]. \tag{3.23}$$

A straightforward calculation yields:

$$W_{j_nj_{n-1}}^{(0)}(\omega)=-\frac{1}{i\omega}\left[1-\sum_m\hat{W}_{mj_{n-1}}^{(j_n)}(\omega)\right], \tag{3.24}$$

$$\hat{D}_{j_1j_0}^{(0)}=\frac{1}{i\omega}\left[\kappa_{j_1j_0}\tilde{\rho}_{j_1j_0}-\sum_m\hat{W}_{j_1m}^{(j_0)}(\omega)\kappa_{mj_0}\tilde{\rho}_{mj_0}\right], \tag{3.25}$$

where $\tilde{\rho}_{mj_0}\equiv\tilde{\rho}^{(j_0)}(q_{j_0m})$.

The distribution of stochastic trajectories Eq. (3.21) can be used to compute any desired statistical property of the system. In Appendix A we use a generating function approach to calculate the probability $P^{(f)}(n;\tau)$ to have n jumps during the time interval τ. This distribution is given by

$$\begin{aligned}P^{(f)}(n;\tau)=\int_{-\infty}^{\infty}\frac{d\omega}{2\pi}\frac{1-e^{-i\omega\tau}}{\omega^2}\sum_{mnm'n'}\kappa_{mn}\tilde{\rho}_{m'n'}\\\times\{[A^{-1}(\omega)-A^{-1}(\omega)B(\omega)A^{-1}(\omega)]\\\times[B(\omega)A^{-1}(\omega)]^{N-1}\}_{mn,m'n'}.\end{aligned} \tag{3.26}$$

A and B are the following tetradic $L^2\times L^2$ matrices:

$$\begin{aligned}A_{mn,m'n'}(\omega)&\equiv\delta_{mm'}\delta_{nn'}+\delta_{mm'}\kappa_{mn'}G_{nn'}^{(m)}(\omega),\\B_{mn,m'n'}(\omega)&\equiv\delta_{mn'}\kappa_{mm'}G_{nm'}^{(m)}(\omega).\end{aligned} \tag{3.27}$$

In the next section we shall apply the general expressions derived here to the simplest case of $A\rightleftharpoons B$ chemical reaction.

IV. RANDOM WALKS AND TRAJECTORIES FOR TWO-LEVEL KINETICS

In the present continuous-time random walk (CTRW) model, the waiting-time distribution of the state $|j_k\rangle$ depends on the state $|j_{k-1}\rangle$ prior to the last flip. This has a simple physical origin. In our model, jumps can only occur at the curve-crossing points q_{mn}, and the jump probability depends on the population at the crossing points. During the waiting time, the Brownian oscillator undergoes diffusion and can

move among the various crossing points. Since the jump to the state $|j_k\rangle$ and $|j_{k-1}\rangle$ occurs at the points $q_{j_k j_{k-1}}$ and $q_{j_{k+1} j_k}$, respectively, the time spent in state $|j_k\rangle$ reflects the flow of population from $q_{j_k j_{k-1}}$. The waiting-time distribution $\hat{W}^{(j_k)}_{j_{k+1} j_{k-1}}(\tau)$ depends therefore on the three states $|j_{k+1}\rangle, |j_k\rangle$, and $|j_{k-1}\rangle$. Stated differently, the $L_c = \frac{1}{2}L(L-1)$ crossing points rather than the L states constitute the sites for stochastic jumps. This is why in Sec. III we expressed the distribution of the number of flips in terms of $L_c^2 \times L_c^2$ superoperators rather than ordinary $L \times L$ operators.

The present $L=2$ case is special since it only has a single crossing point $q_{12}=q_{21}$. The distributions $\hat{W}^{(j_k)}_{j_{k+1} j_{k-1}}$ can be considered as depending on $|j_k\rangle$ only, since given $|j_k\rangle, |j_{k+1}\rangle$, and $|j_{k-1}\rangle$ are uniquely determined from the condition $j_{k+1}=j_{k-1}\neq j_k$. $\hat{W}^{(j)}$ [Eq. (3.19)] and the Green functions $G^{(j)}$ therefore loose their matrix structure as well, and become scalars. This results in an ordinary two-state CTRW model with the waiting-time distribution.

$$W^{(j)}(\tau) = \int_{-\infty}^{\infty} \frac{d\omega}{2\pi} e^{-i\omega\tau} \hat{W}^{(j)}(\omega). \tag{4.1}$$

Equation (3.19) which becomes a scalar rather than a matrix expression immediately gives

$$\hat{W}^{(j)}(\omega) = \frac{\kappa G^{(j)}(\omega)}{1+\kappa G^{(j)}(\omega)}. \tag{4.2}$$

The distribution of number of flips $P^{(f)}(N,\tau)$ [Eq. (3.26)] also simplifies considerably in this case. The superoperators A and B [Eq. (3.27)] act in a two-dimensional space with the basis $|mn\rangle$ represented by $|ab\rangle$ and $|ba\rangle$. Denoting these basis elements $|1\rangle \equiv |ab\rangle, |2\rangle \equiv |ba\rangle$ [Eq. (3.27)] yields

$$\begin{aligned} A_{mn}(\omega) &= \delta_{mn}[1+\kappa G^{(m)}(\omega)], \\ B_{mn}(\omega) &= (1-\delta_{mn})\kappa G^{(m)}(\omega). \end{aligned} \tag{4.3}$$

Substituting Eq. (4.3) into Eq. (3.26) and making use of the fact that the matrices $A(\omega)$ and $B(\omega)$ have only diagonal and off-diagonal components, respectively, we obtain

$$P^{(f)}(2m-1;\tau) = 2\kappa\tilde{\rho}\int_{-\infty}^{\infty} \frac{d\omega}{2\pi} \frac{1-e^{-i\omega\tau}}{\omega^2} \frac{[\hat{W}^{(1)}(\omega)\hat{W}^{(2)}(\omega)]^m}{\kappa^2 G^{(1)}(\omega) G^{(2)}(\omega)}, \tag{4.4}$$

$$P^{(f)}(2m;\tau) = \kappa\tilde{\rho}\int_{-\infty}^{\infty} \frac{d\omega}{2\pi} \frac{1-e^{-i\omega\tau}}{\omega^2} [\hat{W}^{(1)}(\omega)\hat{W}^{(2)}(\omega)]^m \times \left\{ \frac{\hat{W}^{(1)}(\omega)}{[\kappa G^{(1)}(\omega)]^2} + \frac{\hat{W}^{(2)}(\omega)}{[\kappa G^{(2)}(\omega)]^2} \right\}, \tag{4.5}$$

for $m=1,2,\ldots$ and

$$P^{(f)}(0;\tau) = 1 - \kappa\tilde{\rho}\int_{-\infty}^{\infty} \frac{d\omega}{2\pi} \frac{1-e^{-i\omega\tau}}{\omega^2} \times \left[\frac{\hat{W}^{(1)}(\omega)}{\kappa G^{(1)}(\omega)} + \frac{\hat{W}^{(2)}(\omega)}{\kappa G^{(2)}(\omega)} \right], \tag{4.6}$$

where $\tilde{\rho} \equiv \tilde{\rho}_{12} = \tilde{\rho}_{21}$.

The Green functions $G^{(j)}(\omega)$ which enter Eqs. (4.4), (4.5), (4.6) both directly and through $\hat{W}^{(j)}(\omega)$ have the form

$$G^{(j)}(\omega) = \int_0^{\infty} d\tau \exp\{i\omega\tau\} \frac{1}{\sqrt{2\pi}\sigma(\tau)} \times \exp\left\{ -\frac{[\bar{x} - x_j(\tau)]^2}{2\sigma^2(\tau)} \right\}, \tag{4.7}$$

with

$$x_j(\tau) \equiv d_j - (d_j - \bar{x}) e^{-\Lambda\tau}, \tag{4.8}$$

the crossing point

$$\bar{x} \equiv \frac{E_1 - E_2}{2\eta(d_1 - d_2)}, \tag{4.9}$$

and

$$\tilde{\rho} = \frac{1}{\sqrt{2\pi}\tilde{\sigma}} \frac{1}{\exp[(\bar{x}-d_1)^2/2\tilde{\sigma}^2] + \exp[(\bar{x}-d_2)^2/2\tilde{\sigma}^2]}, \tag{4.10}$$

with $\tilde{\sigma}^2 \equiv k_B T/2\eta$.

Equations (4.4)–(4.6) together with Eqs. (4.7)–(4.10) constitute a closed set of expressions for $P^{(f)}(N;\tau)$ in a two-level kinetics. Let us consider first the limiting case where the bath relaxation rate Λ is fast compared with the kinetics. In this case the system can be described by an ordinary rate equation for the level populations rather than by Eq. (2.5) which describes the dynamics of the population wavepackets, and the trajectory has a simple Poisson statistics. To recover this limit we replace $G^{(j)}(\omega)$ by its long-time (i.e., low-frequency) asymptotic form $G_0^{(j)}(\omega)$:

$$G_0^{(j)}(\omega) = -\frac{1}{i\omega} \frac{1}{\sqrt{2\pi}\tilde{\sigma}} \exp\left[-\frac{(\bar{x}-d_j)^2}{2\tilde{\sigma}^2} \right], \tag{4.11}$$

the kinetic rate to go from state m to n now assumes the Marcus form[31]

$$k_{nm} = (1-\delta_{mn}) \frac{\kappa}{\sqrt{2\pi}\tilde{\sigma}} \exp\left[-\frac{(\bar{x}-d_m)^2}{2\tilde{\sigma}^2} \right]. \tag{4.12}$$

Equation (4.12) represents the Marcus rates.[31] Substituting $\tilde{\sigma}^2 = k_B T/2\eta$ and using the expressions for κ [Eq. (3.7)] and $\bar{x}$ [Eq. (4.9)] yields

$$k_{mn} = (1-\delta_{mn}) \frac{2\pi J^2}{\sqrt{4\pi k_B \lambda T}} \exp\left[-\frac{(\Delta G_{mn} + \lambda)^2}{4\lambda k_B T} \right], \tag{4.13}$$

where $\lambda \equiv \eta(d_2-d_1)^2$ is the reorganization energy, and $\Delta G_{mn} \equiv (E_m - \eta d_m^2) - (E_n - \eta d_n^2)$ is the reaction free energy.

Substituting Eq. (4.11) in Eqs. (4.1) and (4.2) yields $W^{(1)}(\omega)=-k_{21}(i\omega-k_{21})^{-1}$ and $W^{(2)}(\omega)=-k_{12}(i\omega-k_{21})^{-1}$. The waiting time distributions Eq. (4.1) and (4.2) become exponential

$$W^{(1)}(\tau)=k_{21}\exp(-k_{21}\tau);\quad W^{(2)}(\tau)=k_{12}\exp(-k_{12}\tau). \tag{4.14}$$

Substituting these in Eqs. (4.5) and (4.6) yields after some straightforward transformations

$$P^{(f)}(2m-1;\tau)=2e^{-k_{21}\tau}\frac{k_{21}k_{12}\tau}{k_{12}+k_{21}}\frac{(k_{12}\tau)^{m-1}(k_{21}\tau)^{m-1}}{(2m-1)!}\times M(m,m;(k_{21}-k_{12})\tau), \tag{4.15}$$

$$P^{(f)}(2m;\tau)=\frac{(k_{12}k_{21}\tau)}{k_{12}+k_{21}}\frac{(k_{12}\tau)^{m-1}(k_{21}\tau)^{m-1})}{(2m)!}\times\{k_{21}\tau e^{-k_{21}\tau}M(m+1,m;(k_{21}-k_{12})\tau)+k_{12}\tau e^{-k_{21}\tau}M(m+1,m;(k_{12}-k_{21})\tau)\}, \tag{4.16}$$

where M denotes the confluent hypergeometric function.

When $k_{12}=k_{21}$ the distributions given by Eqs. (4.15) and (4.16) are Poissonian. Otherwise the statistics described in Eqs. (4.4)–(4.6) represents a convolution of two Poissonians. Deviations from Poisson statistics are noticeable once the bath relaxation rate becomes comparable to or slower than the kinetics, and the simple kinetic description no longer holds. These will be demonstrated in the next section.

V. NUMERICAL RESULTS AND DISCUSSION

To illustrate the two-level kinetics, we consider a symmetric reaction in which the reactant and product free energy is the same, $\Delta G_{12}=0$. The minima of the two potential energy surfaces are equal, i.e., $E_1-E_2=0$, and the position of the minima are $d_1=0.05$ and $d_2=-0.05$. We choose the coupling constant $J=0.003\ \mathrm{cm}^{-1}$, the temperature $T=300$ K, and the vibronic coupling $\eta=5000\ \mathrm{cm}^{-1}$. With this choice of parameters, the Marcus rate becomes $k=4.41\times10^3\ \mathrm{s}^{-1}$. The regularization parameter is set to $\sigma_0^2=\tilde{\sigma}^2/10$, and the relaxation rate Λ is varied between $0.01k$ and $10k$.

The numerical calculations require some care. The integrand in Eq. (4.7) does not vanish at long times. We therefore rewrite Eq. (4.7) by subtracting and adding the asymptotic value of the integrand $C^{(j)}$ under the integral, i.e.,

$$G^{(j)}(\omega)=\int_0^\infty d\tau e^{i\omega\tau}\left[\frac{1}{\sqrt{2\pi}\sigma(\tau)}\times\exp\left\{-\frac{[\bar{x}-x_j(\tau)]^2}{2\sigma^2(\tau)}\right\}-C^{(j)}\right]+C^{(j)}\frac{i}{\omega}, \tag{5.1}$$

where $C^{(j)}=\exp[-(\bar{x}-d_j)^2/2\tilde{\sigma}^2]/\sqrt{2\pi}\tilde{\sigma}$. The integrand now decays to zero, and the numerical computation can be performed by using a standard fast Fourier transform (FFT) routine. We now have

$$G^{(j)}(\omega)=-g^{(j)}(\omega)/i\omega, \tag{5.2}$$

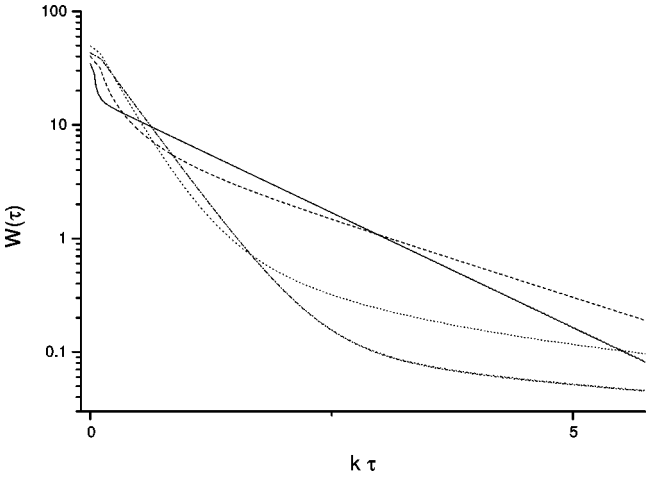

FIG. 1. Waiting time distribution $W(\tau)$ for relaxation rates $\Lambda=10k$ (solid line), $\Lambda=k$ (dashed line), $\Lambda=0.05k$ (dotted line), and $\Lambda=0.01k$ (dashed-dotted line). The other parameters are given in the text.

where

$$g^{(j)}(\omega)=C^{(j)}-i\omega\int_0^\infty d\tau e^{i\omega\tau}\left[\frac{1}{\sqrt{2\pi}\sigma(\tau)}\times\exp\left\{-\frac{[\bar{x}-x_j(\tau)]^2}{2\sigma^2(\tau)}\right\}-C^{(j)}\right]. \tag{5.3}$$

Substituting this expression for into Eq. (4.4), the $1/\omega^2$ factor is cancelled, and we can now compute the expression

$$p^{(f)}(2m-1;\tau)\equiv2\kappa\tilde{\rho}\int_{-\infty}^\infty\frac{d\omega}{2\pi}\times\exp(-i\omega\tau)\frac{[\hat{W}^{(1)}(\omega)\hat{W}^{(2)}(\omega)]^m}{\kappa^2g^{(1)}(\omega)g^{(2)}(\omega)}, \tag{5.4}$$

by using a standard FFT routine, and obtain $P^{(f)}(2m-1;\tau)\equiv p^{(f)}(2m-1;\tau)-p^{(f)}(2m-1;0)$. $P^{(f)}(2m;\tau)$ [Eq. (4.5)] can be calculated in a similar way. The probability for zero jumps [Eq. (4.6)] can be computed as follows. Substituting Eq. (5.2) into Eq. (4.6) gives

$$P^{(f)}(0;\tau)=1-\kappa\tilde{\rho}\int_{-\infty}^\infty\frac{d\omega}{2\pi}\frac{2\sin(\omega\tau/2)}{\omega\exp(i\omega\tau/2)}\times\left[\frac{\hat{W}^{(1)}(\omega)}{\kappa g^{(1)}(\omega)}+\frac{\hat{W}^{(2)}(\omega)}{\kappa g^{(2)}(\omega)}\right]. \tag{5.5}$$

The integrand is regular for $\omega\to0$, and this expression can be easily computed using numerical integration.

By symmetry, the two waiting time distributions coincide: $W^{(1)}(\tau)=W^{(2)}(\tau)\equiv W(\tau)$. Figure 1 shows a logarithmic plot of $W(\tau)$ for fast, intermediate and slow relaxation, $\Lambda=10k$ (solid), $\Lambda=k$ (dashed), $\Lambda=0.05k$ (dotted), and $\Lambda=0.01k$ (dashed-dotted), respectively. We clearly see the expected exponential decay of $W(\tau)$ [Eq. (4.16)] in the limit of fast relaxation, and the increasingly nonexponential behavior for slower relaxation rates.

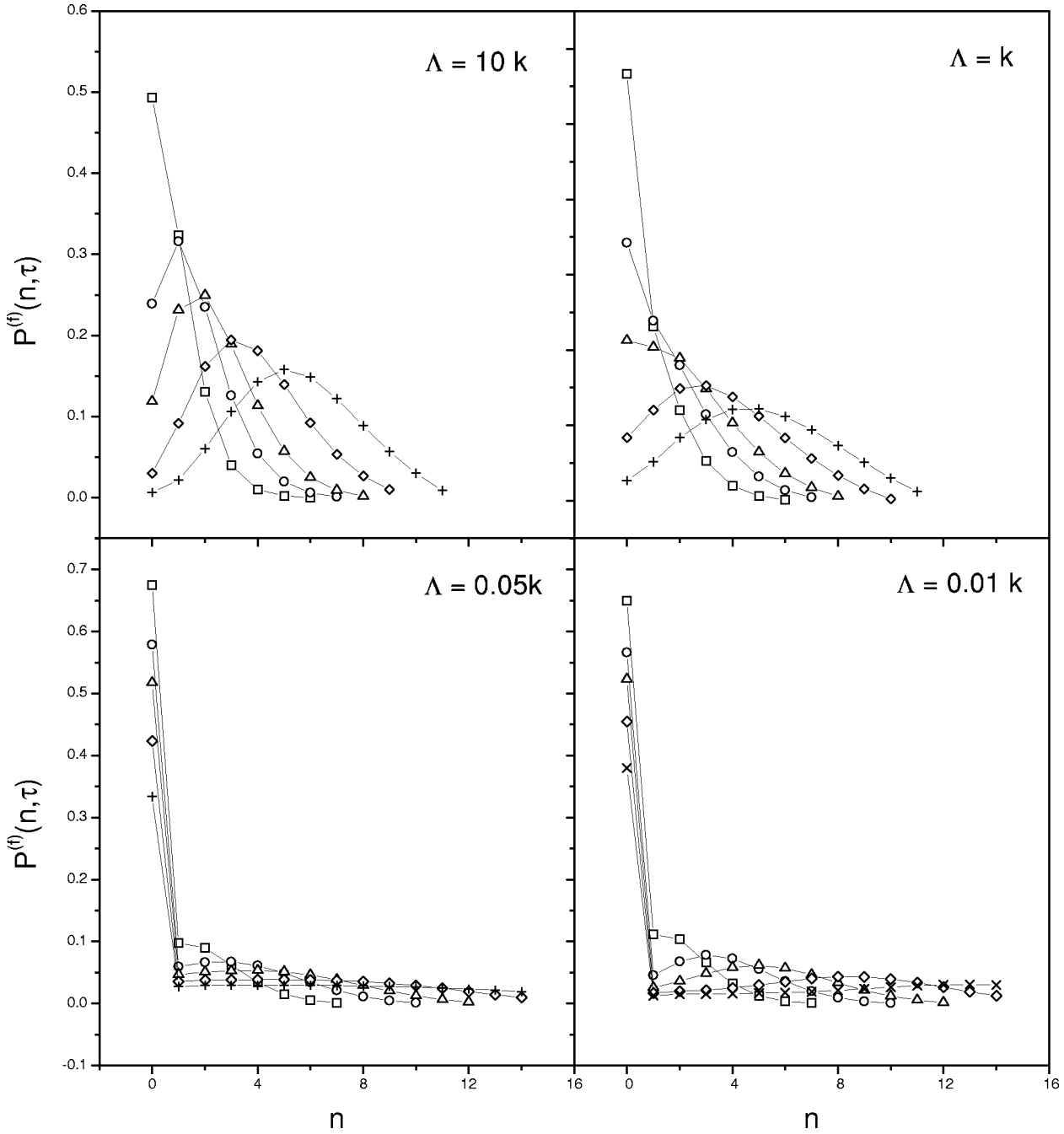

FIG. 2. Probability $P^{(f)}(n;\tau)$ of having n jumps at time τ. The four panels represent different relaxation rates Λ as indicated in each panel. The times $k\tau$ are 0.77 (squares), 1.53 (circles), 2.30 (triangles), 3.83 (diamonds), and 5.75 (crosses).

Figure 2 shows the probability $P^{(f)}(n;\tau)$ of having n jumps for different relaxation rates Λ (as indicated in each panel). The various curves correspond to five values of $k\tau$, represented by squares ($k\tau=0.77$), circles (1.53), triangles (2.30), diamonds (3.83), and crosses (5.75). The connecting lines are added to guide the eye. The fast relaxation ($\Lambda=10k$) limit gives a Poisson distribution, as expected. With decreasing relaxation rate, a strong deviation from Poisson statistics can be clearly discerned. The most pronounced feature is a peak at zero jumps. This can be understood as follows. If a jump occurs and the relaxation rate is fast, then the wavepacket produced at the crossing point is quickly equilibrated. However, in the case of slow relaxation, this wavepacket has a long lifetime at the crossing point, so that the system can jump back and forth several times. Thus, for slow relaxation, we have to think of the system as having a certain probability $P^{(f)}(0;\tau)$ that a jump does not occur, and a probability $1-P^{(f)}(0;\tau)$ that a jump does occur. Due to the long lifetime of the wavepacket at the crossing point, the probability that a jump does occur represents a broad range of the number of jumps n, so that the probability $P^{(f)}(n;\tau)$ for exactly n jumps to occur is fairly small in comparison to $P^{(f)}(0;\tau)$.

The increasing deviation from Poisson statistics with decreasing Λ is further illustrated in Fig. 3, which shows $P^{(f)}(n;\tau)$ as a function of time $k\tau$ for different values of Λ

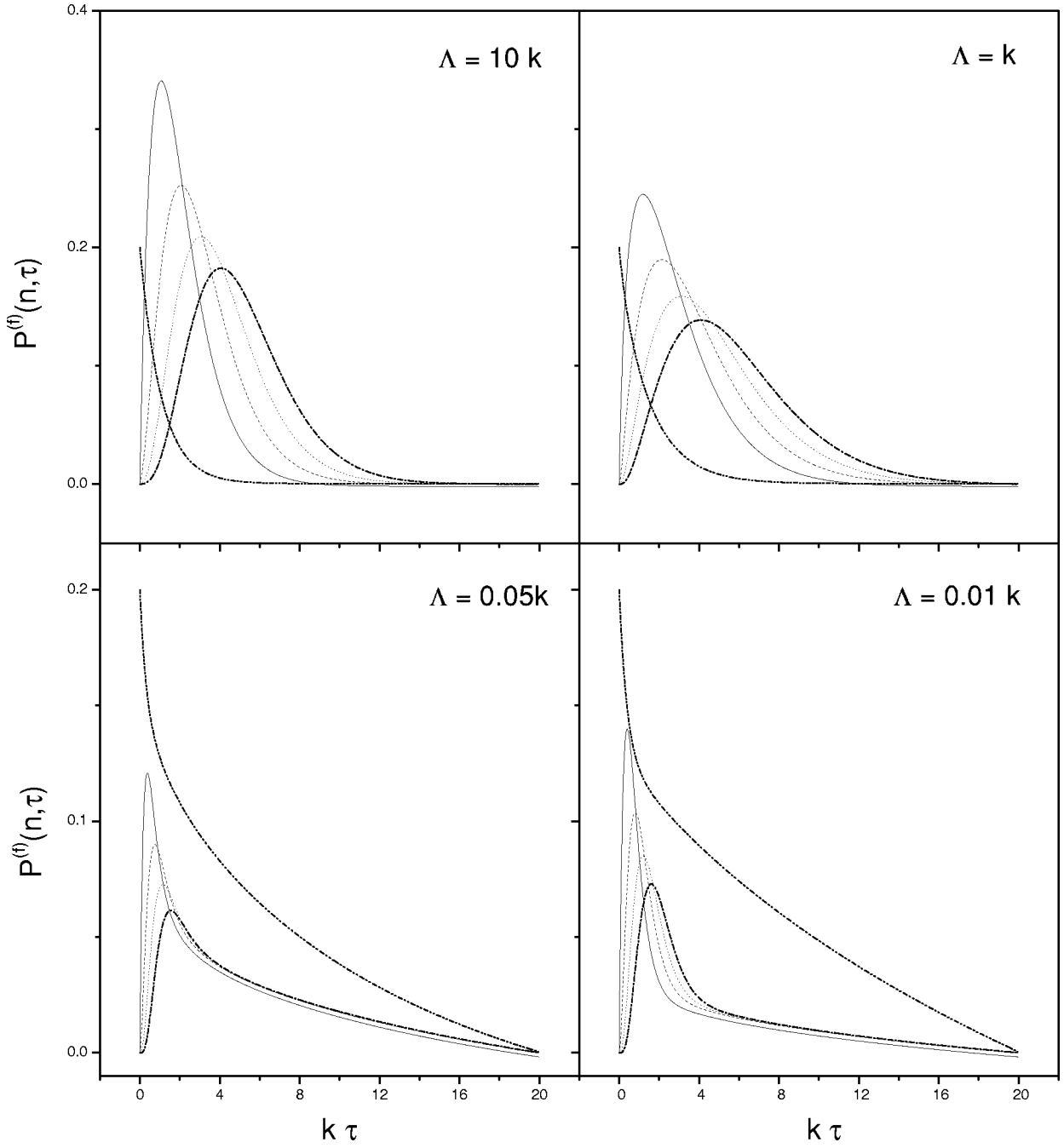

FIG. 3. Probability $P^{(f)}(n;\tau)$ of having n jumps at time τ, plotted vs τ. The four panels represent different relaxation rates Λ as indicated in each panel. The number of jumps n are represented by dash-dot-dotted ($n=0$), solid ($n=1$), dashed ($n=2$), dotted ($n=3$), and dash-dotted lines ($n=4$), respectively. The curve for $n=0$ has been reduced in the ordinate direction by a factor of 5.

as in the previous figure. Different numbers of jumps n are represented by dash-dot-dotted ($n=0$), solid ($n=1$), dashed ($n=2$), dotted ($n=3$), and dash-dotted lines ($n=4$), respectively. The curves for $n=0$ have been reduced by a factor of 5. With decreasing Λ the temporal maximum of $P^{(f)}(n;\tau)$ shifts to earlier times, and the function acquires a long tail. With increasing n, the maximum of the curves shifts to later times.

ACKNOWLEDGMENTS

The support of the National Science Foundation through Grants No. CHE-9526125 and No. PHY94-15583, and the Air Force office of scientific research is gratefully acknowledged.

APPENDIX A: DISTRIBUTIONS OF NUMBERS OF FLIPS

The expressions derived in Sec. III [Eqs. (3.21), (3.24), and (3.19)] give the probability P_s of a stochastic trajectory in terms of the Green functions $G_{mn}^{(j)}$ of the Smoluchowski equations. In this appendix we apply these expressions to compute the probability $P^{(f)}(n;\tau)$ to have n jumps during the time interval τ. $P^{(f)}$ is defined by the time-ordered integrals:

$$P^{(f)}(n;\tau)=\int_0^{\tau} d\tau_n \int_0^{\tau_n} d\tau_{n-1} \ldots \int_0^{\tau_2} d\tau_1 \times \sum_{j_0 \ldots j_n} P_s(j_n,\ldots,j_0;\tau_n,\ldots,\tau_1). \quad \text{(A1)}$$

Combining Eqs. (A1) and (3.21) yields

$$P^{(f)}(n;\tau)=\int_{-\infty}^{\infty} \frac{d\omega}{2\pi} \sum_{j_0 \ldots j_n} \hat{W}^{(0)}_{j_n j_{n-1}}(\omega) \times \hat{W}^{(j_{n-1})}_{j_n j_{n-2}}(\omega) \ldots \hat{W}^{(j_1)}_{j_2 j_0}(\omega) \overline{\mathcal{D}}^{(0)}_{j_1 j_0}(\omega) \times \exp(-i\omega\tau). \quad \text{(A2)}$$

The summation allows us to interpret Eq. (A2) as a product of superoperators acting in the space of operators generated by $|i\rangle\langle j|$. This can be obtained directly from Eq. (A2). We will obtain it, however, in an alternative indirect way where the superoperator structure arises more naturally. To that end we introduce the operators $\mathcal{L}\equiv\Sigma_j \mathcal{L}_j$ and $v\equiv\Sigma_{ij} v_{ij}$ which act in the total space of population wavepackets. Defining a family of operators $\mathcal{L}(\varphi)\equiv\mathcal{L}+\varphi v$ parametrized by φ, expanding the operator $\exp[-i\mathcal{L}(\varphi)]$ in powers of φ, and making use of Eqs. (A1) and (2.5) we obtain

$$\mathrm{Tr}\{\exp[-i\mathcal{L}(\varphi)\tau]\tilde{\rho}\}=\sum_{n=0}^{\infty} \varphi^n P^{(f)}(n;\tau). \quad \text{(A3)}$$

This serves as a generating function for the distribution of jumps, and we immediately have

$$P^{(f)}(n;\tau)=\frac{1}{n!}\frac{\partial^n}{\partial\varphi^n}\mathrm{Tr}\{\exp[-i\mathcal{L}(\varphi)\tau]\tilde{\rho}\}|_{\varphi=0}. \quad \text{(A4)}$$

The r.h.s of Eq. (A4) can be evaluated in the following way: The set of wavepackets $\rho^{(m)}(q,\tau)\equiv\rho_{mm}(q,\tau)$ which describe $\exp[-i\mathcal{L}(\varphi)\tau]\tilde{\rho}$ can be obtained by solving the equation

$$\frac{\rho^{(m)}(q,\tau)}{d\tau}=\mathcal{L}^{(0)}_m \rho^{(m)}(q,\tau)+\sum_n \kappa_{mn}\overline{\rho}(q-q_{mn}) \times[\varphi\rho^{(n)}(q,\tau)-\rho^{(m)}(q,\tau)], \quad \text{(A5)}$$

with the initial condition $\rho^{(n)}(q,0)=\tilde{\rho}^{(n)}(q)$. For $\varphi=1$ Eq. (A5) yields Eq. (3.5). Since the Smoluchowski operators $\mathcal{L}^{(0)}_m$ conserve the trace, time integration of Eq. (A5) gives

$$\mathrm{Tr}\{\exp[-i\mathcal{L}(\varphi)\tau]\tilde{\rho}\} =1+\sum_{mn} \kappa_{mn}\int_0^{\tau} d\tau'[\varphi\rho^{(n)}(q_{mn},\tau')-\rho^{(m)}(q_{mn},\tau')]. \quad \text{(A6)}$$

The r.h.s. of Eq. (A6) only involves the values of the wavepackets at the crossing points $\rho^{(n)}_{mn}(\tau')\equiv\rho^{(n)}(q_{mn},\tau')$. These can be expressed in terms of the Green functions $G^{(j)}_{mn}$ using a standard solution of Eq. (A5). In the frequency domain this yields the following equation:

$$\rho_{mn}(\omega)=-\frac{1}{i\omega}\tilde{\rho}_{mn}+\sum_k \kappa_{mk}G^{(m)}_{nk}(\omega) \times[\varphi\rho_{km}(\omega)-\rho_{mk}(\omega)], \quad \text{(A7)}$$

where we have introduced the notation $\rho_{mn}(\omega)\equiv\rho^{(m)}_{mn}(\omega)$.

Equation (A7) can be solved by introducing the superoperators Eq. (3.27). Substituting the solution of Eq. (A7) into Eq. (A6) we obtain

$$\mathrm{Tr}\{\exp[-i\mathcal{L}(\varphi)\tau]\tilde{\rho}\} =1-\int_{-\infty}^{\infty}\frac{d\omega}{2\pi}\frac{1-e^{-i\omega\tau}}{\omega^2}(1-\varphi)\sum_{mnm'n'} \kappa_{mn} \times[A(\omega)-\varphi B(\omega)]^{-1}_{mn,m'n'}\tilde{\rho}_{m'n'}. \quad \text{(A8)}$$

Combining Eqs. (A8) and Eq. (A4) we finally get Eq. (3.26).

[1] W. E. Moerner and M. Orrit, Science **283**, 1670 (1999).
[2] X. S. Xie and J. K. Trautman, Annu. Rev. Phys. Chem. **49**, 441 (1998).
[3] S. Nie and R. N. Zare, Annu. Rev. Biophys. Biomol. Struct. **26**, 567 (1997).
[4] T. Plakhotnik, E. A. Donley, and U. P. Wild, Annu. Rev. Phys. Chem. **48**, 181 (1997).
[5] W. E. Moerner and T. Basche, Angew. Chem. Int. Ed. Engl. **32**, 457 (1993); W. E. Moerner, Science **265**, 46 (1994); Acc. Chem. Res. **29**, 563 (1996).
[6] M. Orrit, J. Bernard, R. Brown, and B. Lounis, *Progress in Optics*, edited by E. Wolf (Elsevier, Amsterdam, 1996); S. Weiss, Science **283**, 1676 (1999).
[7] T. Basche, W.E. Moerner, M. Orrit, and U. P. Wild, *Single Molecule Optical Detection, Imaging and Spectroscopy* (Verlag-Chemie, Weinheim, Germany, 1997).
[8] T. Joo, Y. Jia, J.-Y. Yu, D. M. Jonas, and G. R. Fleming, J. Chem. Phys. **100**, 2399 (1996); R. Jiminez, F. van Mourik, and G. R. Fleming, *ibid.* **101**, 7350 (1997).
[9] N. R. S. Reddy, G. J. Small, M. Silbert, and R. Picorel, J. Chem. Phys. **181**, 391 (1991); N. R. S. Reddy, R. Picorel, and G. J. Small, *ibid.* **96**, 9458 (1992).
[10] T. Schmidt, G. J. Schutz, W. Baumgartner, H. J. Gruber, and H. Schindler, J. Phys. Chem. **99**, 17662 (1995).
[11] R. M. Dickson, D. J. Norris, Y.-L. Tzeng, and W. E. Moerner, Science **274**, 966 (1996).
[12] X.-H. Xu and E. S. Yeung, Science **275**, 1066 (1997).
[13] T. Ha, J. Glass, T. Enderle, D. S. Chemla, and S. Weiss, Phys. Rev. Lett. **80**, 2093 (1998).
[14] H. P. Lu and X. S. Xie, Nature (London) **385**, 143 (1997).
[15] S. Wennmaim, L. Edman, and R. Rigler, Proc. Natl. Acad. Sci. USA **94**, 10641 (1997).
[16] D. A. Vanden Bout, W.-T. Yip, D. Hu, D.-K. Fu, T. M. Swager, and P. Barbara, Science **277**, 1074 (1997).
[17] H. P. Lu, L. Xun, and X. S. Xie, Science **282**, 187 (1998).
[18] P. D. Reilly and J. Skinner, J. Chem. Phys. **101**, 95 (1994).
[19] G. Zumofen and J. Klafter, Chem. Phys. Lett. **219**, 303 (1994).
[20] Y. Tanimura, H. Takano, and J. Klafter, J. Chem. Phys. **108**, 1851 (1998).
[21] R. Kubo, J. Phys. Soc. Jpn. **9**, 93 (1954); Adv. Chem. Phys. **15**, 101 (1969); *Fluctuation, Relaxation, and Resonance in Magnetic Systems*, edited by D. TerHaar (Oliver and Boyd, Edinburgh, 1962).
[22] J. Klafter, G. Zumofen, and M. F. Shlesinger, *Proceedings of the Enrico Fermi Varenna School on Complex Systems Course CXXXIV*, edited by F. Mallamace and H. E. Stanley, Vol. 85, 1997; *Fractal Frontiers*, Proceedings of the Fractals 97 Conference, edited by M. Novak and G. Dewey, Vol. 453, 1997; *Levy Flights and Related Topics in Physics*, edited by M. Shlesinger, G. Zaslavsky, and U. Frisch (Springer, New York, 1995), Vol. 196.
[23] R. J. Cook and H. J. Kimble, Phys. Rev. Lett. **54**, 1023 (1985).
[24] W. H. Zurek, Phys. Today, October, 36 (1991); M. Gell-Mann, J. B. Hartle, *in Complexity, Entropy, and the Physics of Information*, edited by W. H. Zurek (Addison-Wesley, California, 1990); J. B. Hartle, *Quantum Cosmology and Baby Universes*, edited by S. Coleman, J. B. Hartle, T.

Piran, and S. Weinberg (World Scientific, Singapore, (1991).
[25] H. J. Carmichael, Phys. Rev. A **56**, 5065 (1997).
[26] K. Molmer, Y. Castin, and J. Dalibard, J. Opt. Soc. Am. B **10**, 524 (1993).
[27] S. Stenholm, Quantum Semiclassic. Opt. **8**, 297 (1996).
[28] R. B. Griffiths, J. Stat. Phys. **36**, 219 (1984); R. Omnes, Rev. Mod. Phys. **64**, 339 (1992).
[29] L. D. Zusman, Chem. Phys. **49**, 295 (1980); **80**, 29 (1993).
[30] M. Sparpaglione and S. Mukamel, J. Chem. Phys. **88**, 3263 (1998).
[31] *Electron transfer*, edited by J. Jortner and M. Bixon (Wiley, New York, 1999).
[32] V. Chernyak and S. Mukamel, J. Chem. Phys. **105**, 4565 (1996).
[33] E. W. Montroll and G. H. Weiss, J. Math. Phys. **6**, 167 (1965).
[34] M. F. Shlesinger, *Encyclopedia of Applied Physics* (VCH, New York, 1996), Vol. 16, p. 45.
[35] J. J. Sakurai, *Modern Quantum Mechanics;* 2nd ed. (Addison-Wesley, Boston, 1994).
[36] J. von Neumann, *Mathematical Foundations of Quantum Mechanics* (Princeton University Press, Princeton, 1955).
[37] A. O. Caldiera and A. J. Leggett, Physica A **121**, 587 (1983); P. Hanggi, P. T. Ralkner, and M. Borkvec, Rev. Mod. Phys. **62**, 251 (1990).
[38] U. Weiss, *Quantum Dissipative Systems* (World Scientific, Singapore, 1992).